The fragmentation of metal-poor massive cores

Andrew Myers and Mark Krumholz, August 31, 2010

Abstract

The collapse of star-forming molecular clouds depends critically on radiation feedback from embedded protostars. In general, radiative heating raises the local Jeans mass, helping the gas resist fragmentation. However, the strength of this effect should depend on the metallicity of the star-forming region through its effect on the dust opacity, which determines the level of coupling between the matter and the radiation. In this project, we perform a series of AMR radiation-hydrodamic simulations with the ORION code to determine what effect varying this coupling has on the star formation process.

Background and Motivation

Observations of the internal structure of infrared dark clouds (IRDCs) using sub-mm interferometry reveal the presence of peaks in the local density distribution termed massive cores. They are measured to have masses in the range of $M \sim 100 M_\odot$, radii of about ~ 0.1 pc, and temperatures of about ~ 20 K (Swift 2009). Because the Jeans mass is

$$M_J \sim \frac{c_s^3}{G^{3/2}\rho^{1/2}} \sim 0.15 M_\odot, \tag{1}$$

where c_s is the isothermal sound speed, G the gravitational constant, and ρ the gas density, these cores should be highly unstable to gravitational collapse, and are thought to be the initial conditions for the formation of single massive stars and massive star systems. Moreover, unlike low-mass star forming cores, massive cores are highly turbulent, with virial ratios of order unity. These factors imply that if the collapse of such an object proceeded

isothermally, you should end up with not one or a few massive objects, but many low mass ones.

The solution to this puzzle (Krumholz (2006), Krumholz & McKee (2008)) is that the collapse is far from isothermal. Once stars begin forming, radiation feedback alters the temperature structure of the gas, giving it the extra pressure support it needs to resist further fragmentation. The importance of this effect depends critically on the surface density of the cores in question. Higher surface densities imply higher accretion luminosities and also a greater ability to trap stellar radiation. The critical surface density at which the radiation feedback effect is strong enough to allow the formation of massive ($> 8 M_\odot$) stars appears to be ~ 1 g cm^{-2}, which is about the surface density observed in known regions of high-mass star formation in the galaxy.

However, as the dominant opacity source in massive cores is that of the interstellar dust grains, the strength of this effect should depend on the gas-to-dust ratio and therefore on the metallicity of the star-forming gas. The metallicity is known to vary by about 2 orders of magnitude between galaxies at $z < 4$ (Pettini 2006), and is practically zero in the star forming environments of the first stars. Because of this wide range of variability, and because the fragmentation of massive cores helps determine the IMF, it is important to gauge the effect of decreased metallicity on core collapse. To do this, we have performed a series of numerical experiments using the AMR radiation-hydrodynamics code ORION. These simulations follow the collapse of a series of massive cores that are identical in every way except for their dust opacities. In what follows, we describe the numerical setup and methods and show some preliminary results.

Numerical Method

The details of the numerical techniques used are described in Krumholz et al. (2010). In brief, the ORION code solves the equations of mass, momentum, and energy conservation with radiative transfer on an AMR grid. The computational domain in discretized into a course grid of N_0^3 cells with L levels of refinement using a refinement ratio of 2. Refinement is triggered whenever 1) a cell exceeds the local Jeans density, given by

$$\rho_J = J^2 \frac{\pi c_s^2}{G \Delta x^2}, \tag{2}$$

where Δx is the cell width and J is taken to be 0.125 (Truelove et al. 1997), and 2) whenever the gradient of the radiation energy density $|\nabla E_{\rm rad}|/E_{\rm rad}$ exceeds 0.15. This allows us to follow the collapse of the cloud and the subsequent radiative heating to resolution of just under 7 AU in all our models.

Whenever a cell at the finest level is tagged for refinement, the code instead places a sink particle on the grid Krumholz et al. (2004), which takes mass from the surrounding cells and radiates with a luminosity L calculated from the protostellar model described in the appendices of Offner et al. (2009). We allow sink particles to merge if they have masses less than 0.05 $M_\odot$ but suppress mergers where both particles are above that mass. This threshold is chosen to roughly correspond to the mass at which second collapse takes place. This may have an impact of the statistics of low mass stars, but since massive stars gain most of their mass via accretion, the impact on the high-mass end of the IMF should be minimal.

The radiation transport is calculated in the grey, flux-limited diffusion approximation with Planck and Rosseland mean opacities κ_p and κ_r taken from Semenov et al. (2003). These opacities have been scaled by a factor $Z_{\rm rel}$ to represent gas with a lower portion of metals. While crude, this is the most straightforward way to vary the coupling between

the matter and radiation, and it is sufficient to gauge the strength of the effect we are considering. Finally, we use a polytropic equation of state with $\gamma = 5/3$, appropriate for a gas of molecular hydrogen in which the rotational degrees of freedom have been frozen out due to the low temperature, although this is usually irrelevant as the thermal properties of the gas are set primarily by stellar radiation.

Initial Conditions

Except for the metallicity variation, the problem setup was kept as similar as possible to Krumholz et al. (2010) and Cunningham et. al. (2010, in prep), to facilitate comparison. We model massive cores as spheres with surface density Σ, mass $M = 300 M_{\odot}$, initial temperature $T = 20$ K, and a power law density profile of

$$\rho(r) \propto r^{-k_{\rho}} \tag{3}$$

where have taken k_{ρ} to be 1.5, consistent with observations (Beuther et al. 2007) and with the theoretical models of McKee & Tan (2003). The radius R of such a core is related to its surface density by

$$\Sigma = \frac{M}{\pi R^2}. \tag{4}$$

We also give the give the cores an initial Gaussian random turbulent velocity profile with $P(k) \sim k^{-2}$ scaled to put them in approximate virial balance. The rms velocity dispersion required to do so is

$$\sigma_v = \sqrt{\frac{GM}{R(2k_{\rho} - 1))}} = \sqrt{\frac{G^2 M \pi \Sigma}{4(k_{\rho} - 1)^2}}. \tag{5}$$

The cores are placed in cubic volume with $L_{\rm box} = 4 \times R$. Around the cores is a background medium with density $\rho_{\rm bg} = 0.01 \times \rho_{\rm edge}$, where $\rho_{\rm edge}$ is the density at the edge of the initial core. To maintain pressure balance, the temperature of the background gas is

set to $T_{\rm bg} = 100 \times T_{\rm core} = 2000$ K. The opacity of the ambient gas is set a tiny value to ensure that it does not interfere with the temperature structure of the collapsing core.

Name	Σ (g cm^{-2})	$Z_{\rm rel}$	R (pc)	σ_v (km s^{-1})	$t_{\rm ff}$ (kyr)	$L_{\rm box}$ (pc)	L	N_0	$N_{\rm L}$	$\Delta x_{\rm L}$ (AU)
A	2	0.05	0.1	3.59	30.2	0.4	6	192	12288	6.71
B	2	0.2	0.1	3.59	30.2	0.4	6	192	12288	6.71
C	2	1.0	0.1	3.59	30.2	0.4	6	192	12288	6.71
D	10	0.2	0.045	5.37	9.03	0.18	5	168	5376	6.85

Table 1: Simulation parameters. All models have $M = 300\ M_{\odot}$.

In table 1, we summarize the parameter values for the different runs. In all cases, the size of the base grid and the number of levels of refinement have been selected to ensure that the peak resolution Δx_l is ~ 7 AU in cases. In general, the numerical factors have been held constant across all the runs, so that any differences between them should be attributable to radiative effects.

Results

The following results are preliminary, pending the completion of all the models. Figure (1) shows projections of the density (left) and density-weighted temperature (right) for run A at a time of 0.3 $t_{\rm ff}$. At this stage in the simulation, a total of ~ 17 solar masses of material has accreted onto stars. A striking difference between this run and the solar metallicity runs of Krumholz et al. (2010) and Cunningham et. al. (2010) is the number of objects created; in this run we have ~ 20 objects at this time, compared to a handful in the other simulations. However, with the most massive star at 6 $M_{\odot}$ and less than 10 % of the core accreted, it seems possible that we will still get a massive star. The simulation needs to run for longer in order to say for sure.

Figure (2) shows the star formation history for the different runs. As not all the runs

Fig. 1.— Column density (g cm^{-2}) (left) and projected, density-weighted gas temperature (K) (right) for model A at 0.3 free fall times. The crosses represent stars with masses greater than $0.05 M_{\odot}$. N-body interactions have begin to disperse some of the stars from the regions of dense gas in which they formed.

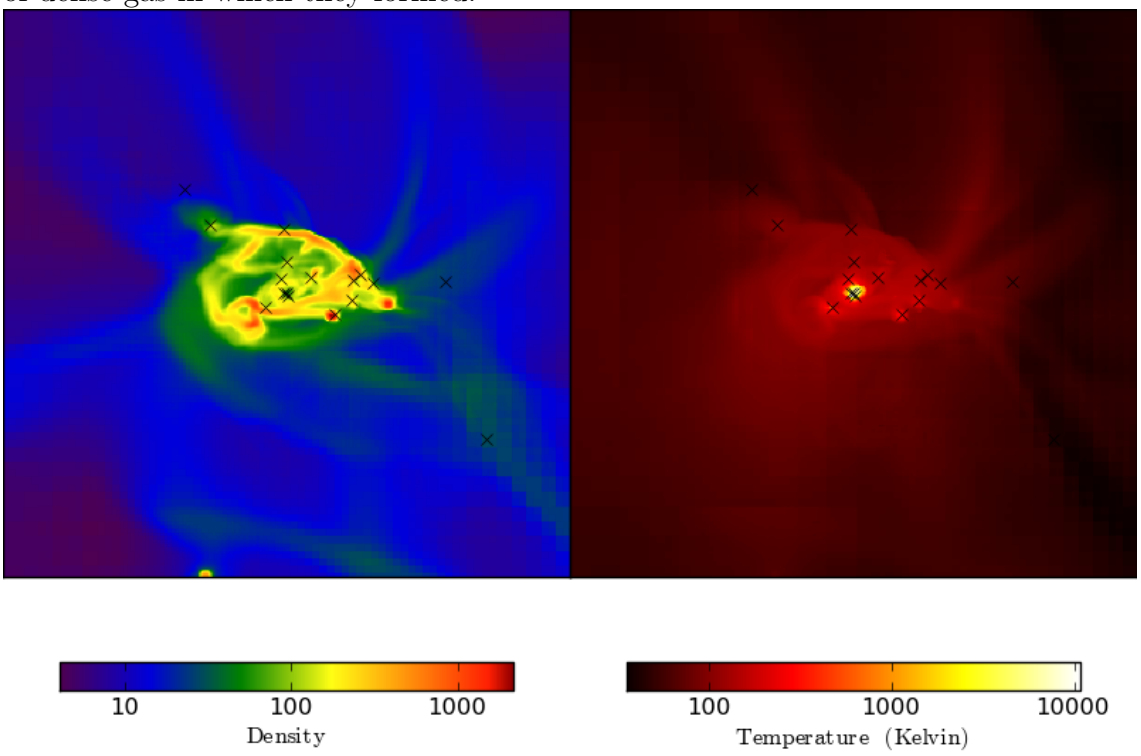

Fig. 2.— Star formation histories for runs A, B, and C. The y-axis shows the total mass in stars in units of $M_{\odot}$, the x-axis shows the simulation time. The three runs are currently a different stages of completion.

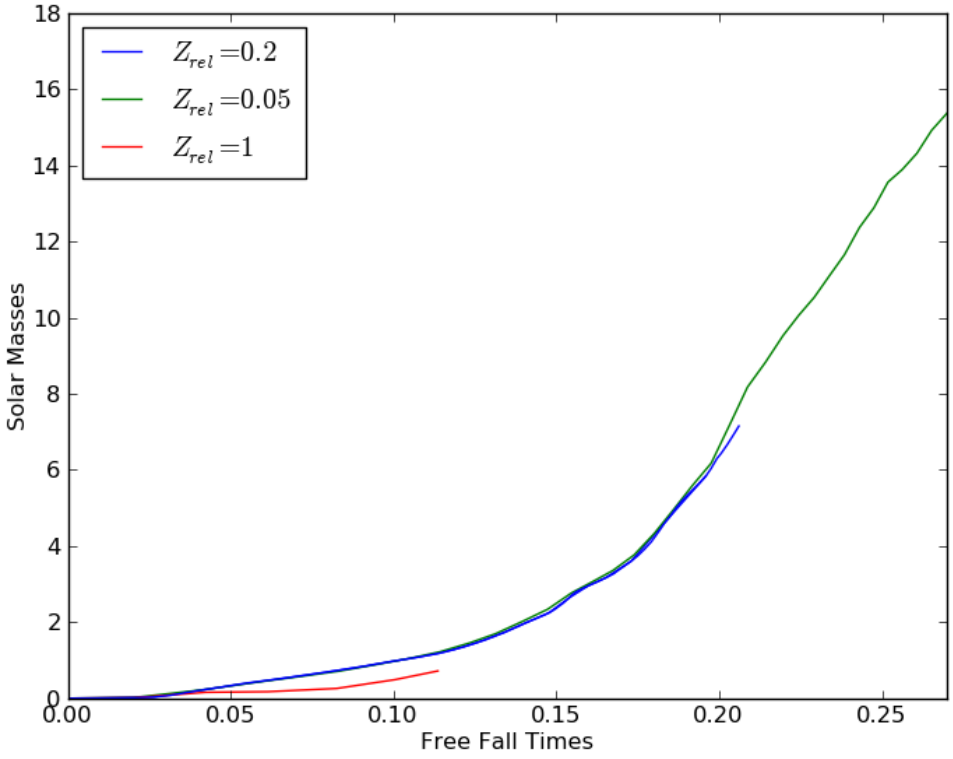

have reached the final time yet, it is too early to draw conclusions about the effect of metallicity on the star formation rate, although we expect that this is set primarily by the rate of global collapse rather than radiative effects and so should be similar between the different runs.

Finally, figure (3) shows the star mass distribution for runs A and B at 0.2 free fall times. At this stage of the simulation, there does not appear to be any quantitative difference between the runs, but this may change as the simulations continue.

Fig. 3.— Fraction ($f(< M)$ of total stellar mass in stars with less than mass M for runs A and B at 0.2 free falls times.

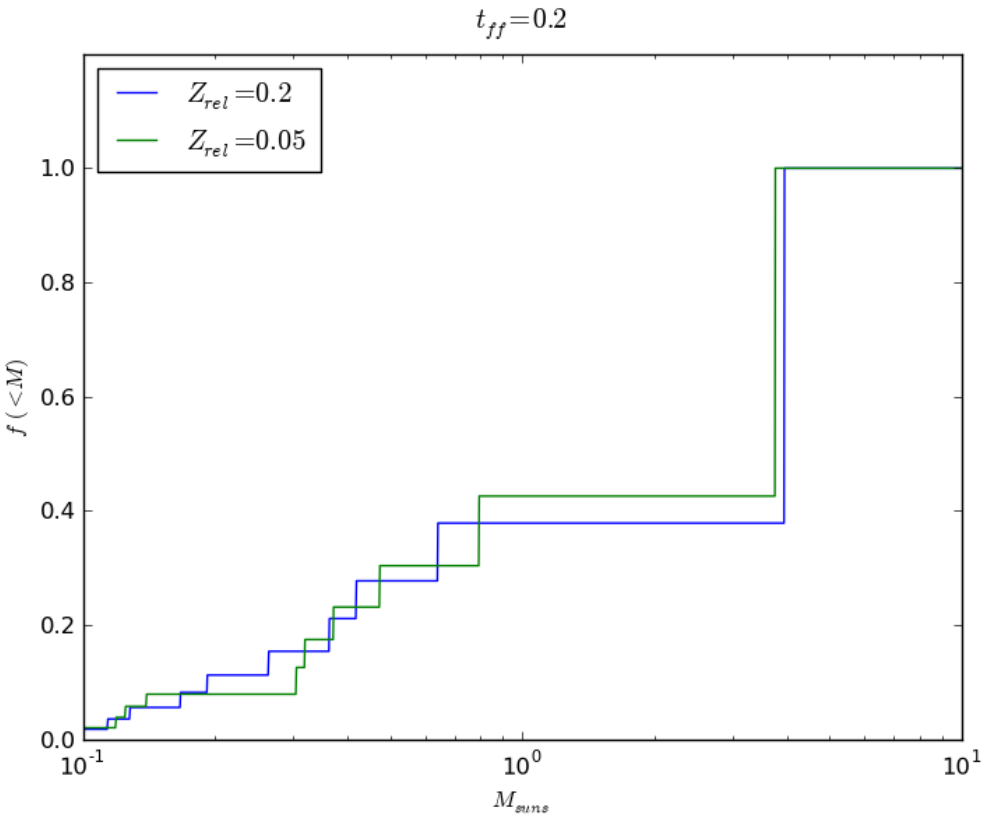

REFERENCES

Beuther, H., Leurini, S., Schilke, P., Wyrowski, F., Menten, K. M., & Zhang, Q. 2007, A&A, 466, 1065

Krumholz, M., McKee, C., & Klein, R. 2004, 611, 399

Krumholz, M. R. 2006, ApJ, 641, L45

Krumholz, M. R., Cunningham, A. J., Klein, R. I., & McKee, C. F. 2010, 713, 1120

Krumholz, M. R., & McKee, C. F. 2008, Nature, 451, 1082

McKee, C. F., & Tan, J. C. 2003, ApJ, 585, 850

Offner, S. S. R., Klein, R. I., McKee, C. F., & Krumholz, M. R. 2009, ApJ, 703, 131

Pettini, M. 2006, in The Fabulous Destiny of Galaxies: Bridging Past and Present, ed. V. Le Brun, A. Mazure, S. Arnouts, & D. Burgarella, 319–+

Semenov, D., Henning, T., Helling, C., Ilgner, M., & Sedlmayr, E. 2003, A&A, 410, 611

Swift, J. J. 2009, ApJ, 705, 1456

Truelove, J. K., Klein, R. I., McKee, C. F., Holliman, II, J. H., Howell, L. H., & Greenough, J. A. 1997, ApJ, 489, L179+

This manuscript was prepared with the AAS LaTeX macros v5.2.